frontiers in Earth Science

ORIGINAL RESEARCH
published: 23 March 2021
doi: 10.3389/feart.2021.641327

Uranium Distribution and Incorporation Mechanism in Deep-Sea Corals: Implications for Seawater [CO_3^{2-}] Proxies

Sang Chen[1,2], Eloise F. M. Littley[3], James W. B. Rae[3], Christopher D. Charles[4] and Jess F. Adkins[2]*

[1] School of Oceanography, Shanghai Jiao Tong University, Shanghai, China, [2] Division of Geological and Planetary Sciences, California Institute of Technology, Pasadena, CA, United States, [3] School of Earth and Environmental Sciences, University of St. Andrews, St. Andrews, United Kingdom, [4] Scripps Institution of Oceanography, University of California, San Diego, La Jolla, CA, United States

A conservative element in seawater, uranium is readily incorporated into the aragonitic skeletons of scleractinian corals, making them an important paleoclimate archive that can be absolutely dated with U-Th techniques. In addition, uranium concentrations (U/Ca ratios) in corals have been suggested to be influenced by the temperature and/or carbonate ion concentration of the ambient seawater based on empirical calibrations. Microsampling techniques have revealed strong heterogeneities in U/Ca within individual specimens in both surface and deep-sea corals, suggesting a biological control on the U incorporation into the skeletons. Here we further explore the mechanism of uranium incorporation in coral skeletons with the deep-sea species *Desmophyllum dianthus*, an ideal test organism for the biomineralization processes due to its relatively constant growth environment. We find a negative correlation between bulk coral U/Ca and temperature as well as ambient pH and [CO_3^{2-}] that is consistent with previous studies. By sampling the growth bands of individual corals, we also find a twofold change in U/Ca within individual corals that is strongly correlated with the $\delta^{18}O$, $\delta^{13}C$, and other Me/Ca ratios of the bands. A similar correlation between U/Ca and stable isotopes as well as other Me/Ca ratios are observed in bulk deep-sea coral samples. With a numerical coral calcification model, we interpret the U/Ca-stable isotope correlation as a result of changes in uranium speciation in response to internal pH elevations in the extracellular calcifying fluid (ECF) of the corals, and suggest that the $Ca_2UO_2(CO_3)_3(aq)$ complex, the dominant U species in seawater, may be the major species incorporated into the coral skeleton. Therefore, the correlation between U/Ca and ambient [CO_3^{2-}] is likely a result of the response of the biomineralization process, especially the magnitude of internal pH elevation, to the growth environment of the corals. Our data suggest overall lower alkalinity pump rates in corals from low saturation seawater compared to those from high saturation seawater, and possible increases in Ca^{2+} supply from active pumping relative to seawater transport in response to the environmental stress of low saturation.

Keywords: deep-sea corals, uranium, carbonate ion, biomineralization, stable isotopes

OPEN ACCESS

Edited by:
Anne M. Gothmann, St. Olaf College, United States

Reviewed by:
Xinming Chen, Florida State University, United States
Jacek Raddatz, Institute of Geosciences, Faculty of Geosciences and Geography, Goethe University Frankfurt am Main, Germany

****Correspondence:***
Sang Chen
sang@sjtu.edu.cn

Specialty section:
This article was submitted to Biogeoscience, a section of the journal Frontiers in Earth Science

Received: *14 December 2020*
Accepted: *22 February 2021*
Published: *23 March 2021*

Citation:
Chen S, Littley EFM, Rae JWB, Charles CD and Adkins JF (2021) Uranium Distribution and Incorporation Mechanism in Deep-Sea Corals: Implications for Seawater [CO_3^{2-}] Proxies. Front. Earth Sci. 9:641327. doi: 10.3389/feart.2021.641327

INTRODUCTION

The minor and trace element contents (Me/Ca ratios) of biogenic carbonates have been used for paleoclimate reconstructions for decades. Among them, uranium is of interest due to its relatively high concentrations allowing it to be used as a dating tool as well as a geochemical proxy, especially in biogenic aragonites (Broecker, 1963; Edwards et al., 1987; Min et al., 1995; Shen and Dunbar, 1995; Cheng et al., 2000; Cutler et al., 2003; Russell et al., 2004; Robinson et al., 2006; Anagnostou et al., 2011; Keul et al., 2013; Raddatz et al., 2014; Chen T. et al., 2016; DeCarlo et al., 2016). Uranium is soluble in oxic seawater as uranyl-carbonate complexes and is readily incorporated into the aragonite lattice (Langmuir, 1978; Djogić et al., 1986; Reeder et al., 2000, 2001). However, the exact mechanism of uranium incorporation into carbonate minerals is still under debate (Reeder et al., 2000, 2001; Anagnostou et al., 2011; DeCarlo et al., 2015; Chen X. et al., 2016; Chen, 2020), complicating its use as a paleoclimate proxy. The uranium incorporation mechanism is further complicated by more recent discoveries that the dominant uranium species in seawater are actually Ca-UO_2-CO_3 and Mg-UO_2-CO_3 complexes due to their high stability constants in a medium of high ionic strength (Dong and Brooks, 2006; Endrizzi and Rao, 2014; Chen X. et al., 2016).

Early work on surface corals found seasonal variations in U/Ca that track sea surface temperature (Min et al., 1995; Shen and Dunbar, 1995). Through thermodynamic calculations of a simple exchange reaction (UO_2^{2+} directly substituting Ca^{2+} in aragonite), it was found that the negative correlation between coral U/Ca and temperature is mainly a result of the temperature dependence of the carbonate system constants and its resulting influence on the speciation of uranium, rather than the temperature dependence of uranium partitioning into the mineral (Min et al., 1995). As a result, the incorporation of uranium into coral skeletons can also be influenced by changes in the carbonate chemistry of the ambient seawater (Min et al., 1995; Shen and Dunbar, 1995). This has inspired efforts in developing U/Ca in biogenic carbonates as a proxy for seawater carbonate ion concentrations ($[CO_3^{2-}]$), especially in the deep ocean where temperature changes are more limited. Empirical calibrations show that U/Ca in both corals and foraminifera are negatively correlated with seawater $[CO_3^{2-}]$ or pH (Russell et al., 2004; Anagnostou et al., 2011; Inoue et al., 2011; Raitzsch et al., 2011; Keul et al., 2013; Raddatz et al., 2014; Allen et al., 2016). A negative U/Ca-$[CO_3^{2-}]$ correlation was also observed in inorganic aragonite precipitation experiments in seawater, without significant influence from temperature or pH, although the apparent sensitivity of U/Ca to $[CO_3^{2-}]$ is different between laboratory-grown aragonite and coral skeletons (DeCarlo et al., 2015).

Different ideas have been proposed for this negative correlation regarding both the uranium species that gets incorporated into the mineral and the exact incorporation mechanism (Reeder et al., 2000; Anagnostou et al., 2011; DeCarlo et al., 2015; Chen X. et al., 2016; Chen, 2020). In solutions of low ionic strength, $UO_2(CO_3)_3^{4-}$ is the dominant species above pH = 8 and increases in abundance with higher pH (Langmuir, 1978; Djogić et al., 1986). Spectroscopic evidence suggests that uranium in aragonite has the same bonding structure as aqueous $UO_2(CO_3)_3^{4-}$ (Reeder et al., 2000). Therefore, the negative correlation between carbonate U/Ca and seawater $[CO_3^{2-}]$ may be a result of a reduced adsorption efficiency for $UO_2(CO_3)_3^{4-}$ at high $[CO_3^{2-}]$ (Barnett et al., 2000; Anagnostou et al., 2011). Such a model, however, does not account for the more complicated uranium speciation in seawater more recently discovered (Dong and Brooks, 2006; Endrizzi and Rao, 2014; Chen X. et al., 2016). The biomineralization process of the calcifying organisms, especially the internal pH elevation in the calcifying fluid of the organisms (Al-Horani et al., 2003; Zoccola et al., 2004; de Nooijer et al., 2009; Venn et al., 2011; Toyofuku et al., 2017), could bring additional complexity to the U/Ca-$[CO_3^{2-}]$ relation observed in biogenic carbonates without good constraints on the actual carbonate chemistry of the calcifying fluid.

Here we further study the incorporation mechanism of uranium in biogenic aragonite with deep-sea corals as a test organism. Deep-sea corals are well-suited to study the impact of the biomineralization process on geochemical tracers (i.e., "vital effects"), due to their relatively constant growth environment and the large tracer gradient observed in individual specimens (Adkins et al., 2003; Rollion-Bard et al., 2003, 2010; Robinson et al., 2006, 2014; Gagnon et al., 2007). Strong tracer correlations have been found in the skeletons of individual deep-sea corals that can be attributed to a common biomineralization process (Adkins et al., 2003; Gagnon et al., 2007; Chen S. et al., 2018). In particular, the strong correlation between carbon and oxygen isotopes ($\delta^{18}O$ and $\delta^{13}C$) of deep-sea coral skeletons has been quantitatively explained with a process-based coral calcification model, which provides the potential to realistically constrain the carbonate chemistry of the extracellular calcifying fluid (ECF) of the corals (Chen S. et al., 2018). As a result, we can explore the fundamental mechanisms of vital effects in the incorporation of minor and trace elements in corals by making coupled Me/Ca and stable isotope measurements. With a suite of modern *Desmophyllum dianthus* specimens, we show a consistent relation between U/Ca and the stable isotopes ($\delta^{18}O$ and $\delta^{13}C$) as well as other Me/Ca ratios of the skeletons in bulk samples and within individual corals. We then discuss the incorporation mechanism of uranium in corals and its implications for U/Ca as a paleo-$[CO_3^{2-}]$ proxy.

MATERIALS AND METHODS

Sample Preparation

The *D. dianthus* specimens used in this study were either provided by the Smithsonian Museum of Natural History or collected from Seamounts south of Tasmania with the deep submergence vehicle Jason during cruise TN-228 in 2008–2009 on the R/V Thompson. Most corals were collected with tissue remains on them and are therefore considered modern. They span a wide range of geographic locations and environmental

TABLE 1 | Bulk U/Ca of *D. dianthus* used in this study.

Coral ID	Lon (°E)	Lat (°N)	Depth (m)	Temp (°C)[a]	$[CO_3^{2-}]$ (μmol/kg)	This study U/Ca (μmol/mol)	Anagnostou U/Ca (μmol/mol)
19249	−119.5	34.0	274	7.8 ± 0.8	56 ± 2	1.868 ± 0.015[b]	2.04 ± 0.14[c]
BigBeauty	−62.2	−54.7	816	3.6 ± 0.3	101 ± 6	1.996 ± 0.003	
47409	−39.4	−54.5	672.5	1.9 ± 0.3	77 ± 3	2.057 ± 0.008	2.13 ± 0.08
Leda-b	147.3	−44.3	1,460	2.9 ± 0.2	71 ± 3	2.100 ± 0.009	
Leda-t	147.3	−44.3	1,460	2.9 ± 0.2	71 ± 3	2.159 ± 0.005	
Gaia	150.3	−44.8	2,395	2.1 ± 0.1	78 ± 2	2.512 ± 0.008	
83583	−127.8	32.9	464	6.0 ± 0.1	46 ± 1	2.125 ± 0.049	2.33
82065	−129.8	−54.8	585.5	5.3 ± 1.0	108 ± 3	1.357 ± 0.021	1.77 ± 0.05
94071	173.3	−30.7	615	9.0 ± 0.3	111 ± 2	1.884 ± 0.002	
47407D	−129.8	−54.8	549	5.5 ± 1.0	107 ± 3	1.346 ± 0.004	0.93 ± 0.1
84820	−91.6	0.2	806	5.9 ± 0.1	58 ± 2	1.982 ± 0.007	2.01 ± 0.15
62309	−67.7	40.4	521.5	5.7 ± 1.0	102 ± 2	1.312 ± 0.005	1.32 ± 0.08
47394	162.0	−51.0	352	5.7 ± 1.0	122 ± 2	1.566 ± 0.006	
53377	167.8	−51.1	210	7.1 ± 0.5	125 ± 2	1.595 ± 0.007	
48744	9.8	43.3	627.5	13.1 ± 0.1	203 ± 1	1.860 ± 0.004	
80404	−4.2	35.4	395	13.2 ± 0.1	184 ± 1	1.600 ± 0.006	
80358	−7.8	48.0	358	11.2 ± 0.1	145 ± 3	1.434 ± 0.006	0.85 ± 0.01
47413A	167.6	−50.6	421	6.8 ± 0.4	123 ± 3	1.492 ± 0.010	1.79
Titan-b	147.3	−44.4	2,066	2.4 ± 0.2	75 ± 2	1.656 ± 0.006	
Titan-t	147.3	−44.4	2,066	2.4 ± 0.2	75 ± 2	1.965 ± 0.003	
97275	117.6	21.7	421	9.0 ± 0.4	142 ± 4	1.424 ± 0.002	

[a] Uncertainties in temperature and $[CO_3^{2-}]$ are estimated from multiple stations in the vicinity of the coral growth sites in the GLODAP v2.0 database. [b] 1σ errors calculated from measurements of different powder aliquots of individual corals. [c] Data and errors as originally reported in Anagnostou et al. (2011). Only corals that were measured in both studies are listed in this column.

conditions (**Table 1**). The environmental conditions of the corals are estimated from nearby stations in the GLODAP v2 database (Key et al., 2015; Olsen et al., 2016) with Ocean Data View (**Table 1**). The carbonate chemical speciation of the ambient seawater is calculated with alkalinity and dissolved inorganic carbon (DIC) in the GLODAP v2 database using CO2SYS, with carbonate chemistry constants from Millero (2010) and in-situ estimates of silicate and phosphate concentrations for each coral.

For bulk coral samples, a small piece containing both the septa and theca was removed from the coral calice. After physically abrading the outer surface, the coral piece was rinsed in ethanol and DI water, dried with compressed air, and crushed into fine powder with mortar and pestle, before chemical processing and geochemical measurements. A few to tens of milligrams of powder were collected for each coral. Different aliquots of the same powder sample were used for stable isotope and Me/Ca measurements.

To study the tracer variability within individual corals, we also sampled growth features in cross sections of the coral skeletons with a Merchantek micromill system, with a method similar to Adkins et al. (2003) and Gagnon et al. (2007). To generate coupled Me/Ca and stable isotope measurements on the same samples, we micromilled growth bands that are typically 100 μm wide, 200 μm deep, and 1–3 mm long. This allowed us to collect 30–100 μg of powder for stable isotope measurements and 50–200 μg of powder for Me/Ca measurements of the same growth band, and directly compare the distribution patterns in different tracers.

Geochemical Analysis

The stable isotopes were measured at Scripps Institution of Oceanography using a Thermo MAT 253 mass spectrometer equipped with a Kiev IV carbonate preparation device. The samples were measured against an in-house reference gas with an isotopic composition originally calibrated to the Vienna Pee Dee Belemnite (VPDB) scale through the NBS-17 gas standard. The carbonate samples were further calibrated to the VPDB scale with the NBS-19 carbonate standard. The long-term reproducibility (1σ) for carbonate measurements in the mass range employed here is 0.03‰ for $\delta^{13}C$ and 0.08‰ for $\delta^{18}O$.

The Me/Ca ratios of the samples were measured in two different labs at the University of St. Andrews and the California Institute of Technology. Measurements of the micromilled samples were split between the two labs, while all the bulk samples were measured at Caltech. With a cleaning test at University of St. Andrews, we found minimal impact of a two-step chemical cleaning (0.1 M NH_4OH+1% H_2O_2 and 0.0005 M HNO_3) on measured U/Ca compared to uncleaned powder from the same coral sample. As a result, the samples were directly dissolved in 5% HNO_3 before Me/Ca analyses. Dilutions of the primary solutions (1:100 at St. Andrews, 1:40 at Caltech) were made to check for $[Ca^{2+}]$ with ^{48}Ca intensity on the mass spectrometer, after which 1 mM $[Ca^{2+}]$ secondary solutions were made for the Me/Ca measurements. The measurements were performed on an Agilent 7500a ICP-MS at St. Andrews, and an Agilent

7500cx ICP-MS at Caltech. Multiple elements were collected during the analyses, including Li, B, Mg, Ca, Mn, Sr, Cd, Ba, and U. The same method was used for the bulk and micromilled samples. This paper specifically focuses on uranium due to its complex speciation as compared to other metal cations. Spatial distributions of other elements in deep-sea coral skeletons are also presented to make cross correlations with uranium, but the detailed mechanisms of these elements will be discussed elsewhere.

The U/Ca ratios of the *D. dianthus* samples were calibrated with well characterized in-house multi-element standards with compositions similar to biogenic carbonates. Coral standard Jcp-1 was measured with the samples to check for the accuracy of the measurements. We obtained U/Ca ratios of 1.192 ± 0.012 μmol/mol (N = 3) at St. Andrews and 1.188 ± 0.005 μmol/mol (N = 15) at Caltech, both within uncertainty of the interlab calibration value of 1.192 ± 0.045 (1σ) μmol/mol (Hathorne et al., 2013), suggesting our U/Ca measurements are accurately calibrated with sub-percent precision.

Coral Calcification Modeling

The goal of this study is to couple stable isotopes and U/Ca to study the uranium incorporation mechanism. The coral calcification model developed by Chen S. et al. (2018) for stable isotopes is used to constrain the carbonate chemistry of the ECF of the corals together with the stable isotope measurements. The model can quantitatively explain all the $\delta^{18}O$ and $\delta^{13}C$ features in deep-sea corals in the framework of internal pH elevation modulated by the enzyme carbonic anhydrase (Chen S. et al., 2018). As a result, we expect the model to realistically simulate the carbonate chemistry of the ECF of the corals corresponding to a given stable isotope measurement.

The incorporation of minor and trace elements (with Mg^{2+} as an example) into the coral skeleton can be modeled with the following equations:

$$\frac{d[Ca]_{ECF}}{dt} = \frac{1}{\tau_{sw}}([Ca]_{sw} - [Ca]_{ECF}) + \frac{1}{2} f_{Ca} \frac{F_{Alk}}{z} - \frac{F_{CaCO_3}}{z} \quad (1)$$

$$\frac{d[Mg]_{ECF}}{dt} = \frac{1}{\tau_{sw}}\left([Mg]_{sw} - [Mg]_{ECF}\right) - \frac{1}{z} F_{CaCO_3} D_{Mg} \frac{[Mg]_{ECF}}{[Ca]_{ECF}} \quad (2)$$

Both equations include a seawater flushing term with a timescale of τ_{sw}. The time scale of seawater turnover should be the same for all geochemical tracers, and is constrained to be a few minutes for *D. dianthus* based on the stable isotopes (Chen S. et al., 2018). For Ca^{2+}, there is an additional source from the alkalinity pump (F_{Alk}) by membrane bond Ca-ATPase. The f_{Ca} term in the alkalinity pump flux represents the fraction of the total alkalinity flux from Ca^{2+} pumping, and accounts for the fact that other forms of alkalinity pumps have been described in corals (Jokiel, 2013; Barott et al., 2015; Barron et al., 2018). Ca^{2+} is removed from the ECF by aragonite precipitation (F_{CaCO_3}), with z being the thickness of the ECF (10 μm) to convert fluxes into concentration changes. For Mg^{2+}, the only source is from seawater flushing, and the sink term is co-precipitation with aragonite with a distribution coefficient of D_{Mg} [$D_{Mg} = (Mg/Ca)_{coral}/(Mg/Ca)_{ECF}$].

As a trace element, the speciation of uranium is dominated by the major ions and the carbonate system. With the carbonate chemistry of the ECF constrained by the stable isotope measurements and the model, we can calculate the corresponding uranium speciation to simulate its incorporation process, and therefore study its incorporation mechanism into coral skeletons. To calculate uranium speciation, we use stability constants determined for high ionic strength conditions from Guillaumont et al. (2003) and Endrizzi and Rao (2014). As with Ca and Mg, the incorporation of uranium into the coral skeleton can be modeled with the equation:

$$\frac{d[U]_{ECF}}{dt} = \frac{1}{\tau_{sw}}([U]_{sw} - [U]_{ECF}) - D_U \frac{\chi_U [U]_{ECF}}{[Ca]_{ECF}} \frac{F_{CaCO_3}}{z} \quad (3)$$

Here we introduce the term χ_U as the fraction of the uranium species that gets incorporated into the coral skeleton in total uranium, and test different incorporation mechanisms with the uranium speciation calculations. Following the definition of χ_U, the U/Ca of the coral aragonite can be calculated as:

$$(U/Ca)_{coral} = D_U \frac{\chi_U [U]_{ECF}}{[Ca]_{ECF}} \quad (4)$$

We note that there are different definitions of D_U in previous inorganic precipitation experiments regarding whether the denominator should be $[Ca^{2+}]$ or $[CO_3^{2-}]$ in the U/Ca ratio (Meece and Benninger, 1993; Gabitov et al., 2008; Raddatz et al., 2014; DeCarlo et al., 2015). We choose $[Ca^{2+}]$ because it is more commonly used in the literature, and uranium most likely substitutes for calcium in the aragonite lattice regardless of the species that is preferentially incorporated (Min et al., 1995; Reeder et al., 2000). Together with the stable isotopes, major ion concentrations and the corresponding carbonate chemistry, we can calculate the steady state $[U]_{ECF}$ and U/Ca of the coral skeleton.

RESULTS

Empirical Tracer Calibration of Bulk Samples

Figure 1 shows plots of bulk *D. dianthus* U/Ca with temperature and carbonate chemistry of the ambient seawater. We see that coral U/Ca is negatively correlated with temperature, seawater $[CO_3^{2-}]$ and pH, consistent with previous studies (Min et al., 1995; Shen and Dunbar, 1995; Anagnostou et al., 2011; Inoue et al., 2011; Raddatz et al., 2014). The correlation with $[CO_3^{2-}]$ (R = −0.70, p < 0.001) is stronger than with pH (R = −0.66, p = 0.002) and temperature (R = −0.55, p = 0.015), although all three are statistically significant. However, we observe a wide range of scatter in these correlations that is similar to the data collected by Anagnostou et al. (2011) with laser ablation ICP-MS, despite using different analytical methods

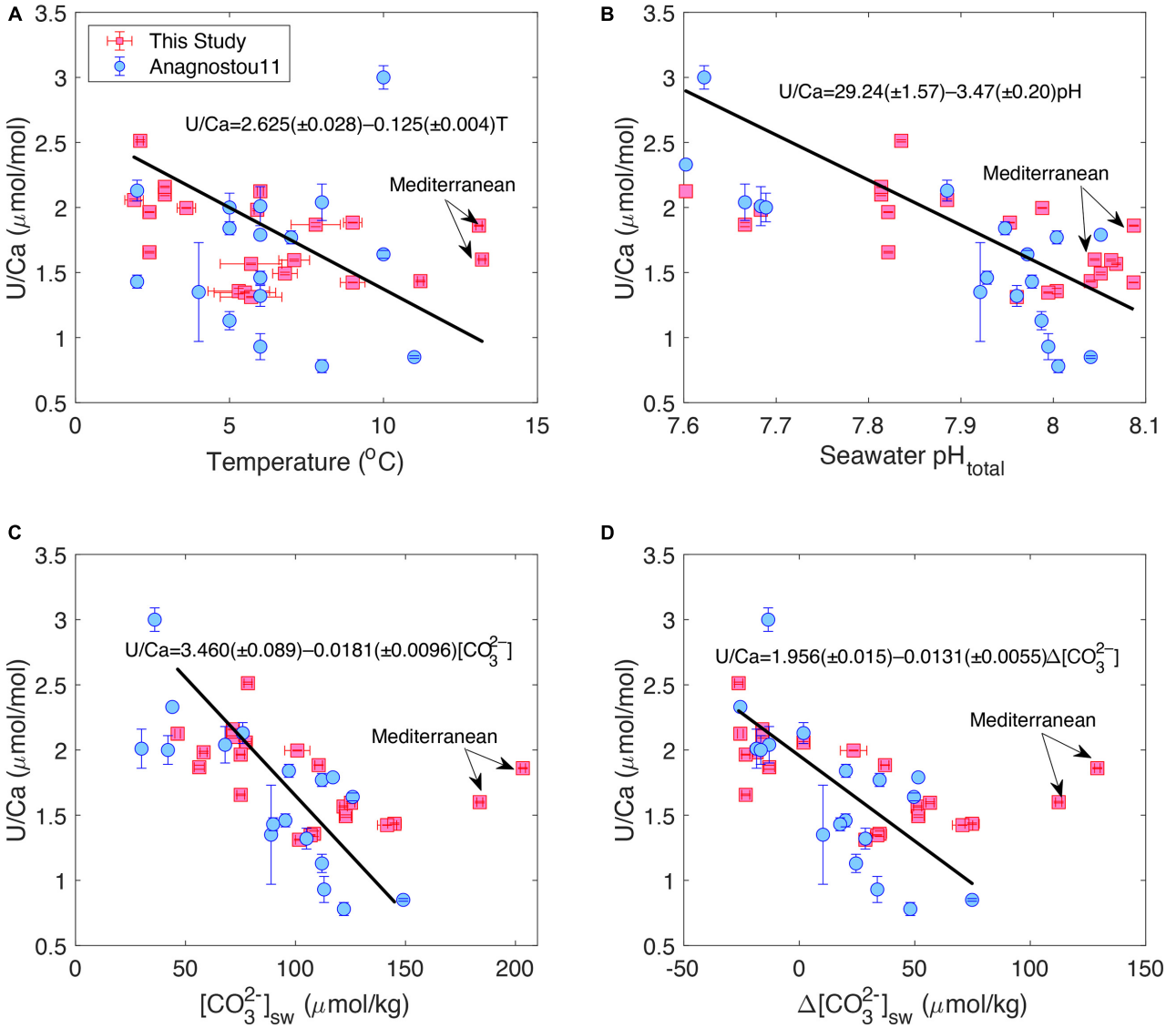

FIGURE 1 | Correlations between bulk *D. dianthus* U/Ca with **(A)** temperature, **(B)** seawater pH, **(C)** seawater [CO_3^{2-}], and **(D)** $\Delta[CO_3^{2-}]$. Red squares are from this study and blue circles are from Anagnostou et al. (2011) with 1σ error bars. The black lines show linear fits to the data in this study considering uncertainties in both environmental estimates and U/Ca measurements following York et al. (2004). Two corals from the Mediterranean Sea are excluded from the linear fits.

and calibration standards that could cause measurement offsets in the same corals (**Table 1**). In our sample set, two corals from the Mediterranean Sea seem to deviate from the U/Ca-[CO_3^{2-}] trend defined by other corals, suggesting possible changes in their biomineralization process in a special environmental setting (**Figure 1B**). When these two corals are excluded, the U/Ca-[CO_3^{2-}] relation we obtained is also statistically indistinguishable from the one found by Anagnostou et al. (2011). We also find that replacing [CO_3^{2-}] with $\Delta[CO_3^{2-}]$ ($[CO_3^{2-}]_{in-situ}-[CO_3^{2-}]_{saturation}$) slightly improves the U/Ca calibration ($R = -0.75$, $p < 0.001$), although the scatter is similar with [CO_3^{2-}] and $\Delta[CO_3^{2-}]$ (**Figures 1C,D**). No clear correlations are found for U/Ca with other environmental conditions.

Tracer Distribution in Individual *Desmophyllum dianthus*

Figure 2 shows an example of the distribution of stable isotopes and some Me/Ca ratios from the micromilled samples in coral 47394. As with previous studies, we find a relatively wide range of tracer variability within a single *D. dianthus* specimen (Adkins et al., 2003; Robinson et al., 2006; Gagnon et al., 2007; Case et al., 2010; Stewart et al., 2016). In a single septum of 47394, we see a 3.5‰ range in $\delta^{18}O$, an 8‰ range in $\delta^{13}C$, a 5% change in Sr/Ca, a 24% change in B/Ca, and almost twofold changes in Mg/Ca and U/Ca (**Figure 2**). Similar ranges of tracer variability are observed in other corals we sampled. In general, the magnitude of tracer variability we observe in individual corals is smaller

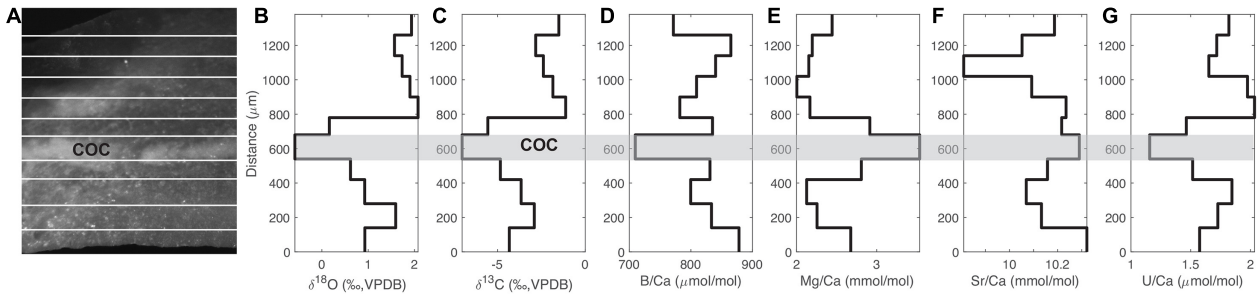

FIGURE 2 | Distribution of isotopes and Me/Ca ratios with growth bands in coral 47394. **(A)** Reflected light image of a thick section of the coral septum that was micromilled, with white lines showing the micromilled bands. There is a COC band in the middle. **(B–G)** Transects of $\delta^{18}O$, $\delta^{13}C$, B/Ca, Mg/Ca, Sr/Ca, and U/Ca of the micromilled bands. The gray bar marks the COC band.

than previous studies. For U/Ca in particular, Robinson et al. (2006) observed threefold U/Ca changes in individual *D. dianthus* with a neutron bombardment and fission track counting method. The narrower range in our data is most likely a result of the micromilling procedure, which sampled relatively large amounts of powder for both stable isotopes and Me/Ca measurements and caused significant spatial averaging, compared to methods used in previous studies. However, the tracer variability we were able to retrieve still covers a sufficiently large gradient that can be used to infer the underlying biomineralization process. We chose this spatial averaging so that measurements of Me/Ca ratios and of stable isotopes could be made on the exact same powder while still preserving the natural banding resolution.

As with previous observations, we also see distinct isotope and Me/Ca compositions in the center of calcification (COC) bands in deep-sea corals, including depletions in $\delta^{18}O$, $\delta^{13}C$, B/Ca U/Ca, and enrichment in Mg/Ca (Adkins et al., 2003; Blamart et al., 2007; Gagnon et al., 2007; Case et al., 2010; Stewart et al., 2016). There is no distinct Sr/Ca change in the COC, also consistent with previous work (Gagnon et al., 2007; Stewart et al., 2016). Such tracer correlations can be used to infer whether the distinct composition of COCs can be explained with the same biomineralization mechanism as the fibrous secondary aragonite.

U/Ca Correlations With Other Tracers

The distribution of tracers with growth bands points toward strong tracer correlations in individual *D. dianthus* skeletons. This paper focuses on uranium, and the correlations between other tracers will be discussed elsewhere. **Figure 3** shows U/Ca correlations with Mg/Ca, Sr/Ca, $\delta^{18}O$, and $\delta^{13}C$ in micromilled bands of individual *D. dianthus*. There is generally a negative correlation between Mg/Ca and U/Ca, and positive correlations for U/Ca with Sr/Ca, $\delta^{18}O$ and $\delta^{13}C$. The COCs may have different tracer correlations from the secondary aragonite, but it is not obvious from the data we collected, which could be a result of the spatial averaging during the micromilling process. Coral 48744 from the Mediterranean Sea shows limited tracer variability in the area we sampled, but still exhibits similar tracer correlation patterns as other corals. The correlations we observe between Mg/Ca, Sr/Ca, and U/Ca are consistent with previous studies of deep-sea corals as well as surface corals (Sinclair, 2005; Gagnon et al., 2007; Raddatz et al., 2014; DeCarlo et al., 2016; Stewart et al., 2016). By coupling Me/Ca ratios with stable isotopes, we also document for the first time the strong positive correlations between U/Ca, $\delta^{18}O$, and $\delta^{13}C$. Given our interpretation of the stable isotopes in deep-sea corals (Adkins et al., 2003; Chen S. et al., 2018), such correlation suggests a decrease in uranium incorporation into the coral skeletons as the alkalinity pump rate is increased in the ECF.

In addition to the micromilled growth bands in individual corals, we also observe strong tracer correlations in our bulk coral samples (**Figure 4**) that are similar to the micromilled samples (**Figure 3**). For U/Ca-Mg/Ca and U/Ca-$\delta^{18}O$, there seems to be a single correlation trend in the bulk samples that is consistent with the micromilled samples in individual corals (**Figures 4A,C**). However, corals from supersaturated and undersaturated seawater show different ranges in tracer values. Corals from undersaturated seawater generally have low Mg/Ca, high U/Ca and enriched $\delta^{18}O$ values and vice versa (**Figures 4A,C**). For U/Ca-Sr/Ca, no clear correlation is observed when all the corals are considered. However, corals from undersaturated seawater exhibit positive U/Ca-Sr/Ca correlations that are similar to the micromill data, while corals from supersaturated seawater do not show a clear U/Ca-Sr/Ca correlation (**Figure 4B**). For U/Ca and $\delta^{13}C$, two separate correlation trends are observed in the bulk data (**Figure 4D**). Corals from warm ($T > 5°C$) supersaturated seawater define a U/Ca-$\delta^{13}C$ relation with a shallower slope, while the other corals define a steeper U/Ca-$\delta^{13}C$ slope. Most of the corals on the steep U/Ca-$\delta^{13}C$ trend live in undersaturated seawater, with two corals from supersaturated seawater at low temperatures ($T < 5°C$). The separation in U/Ca-$\delta^{13}C$ slopes can also be seen in the micromill data, where there is a wider spread in the U/Ca-$\delta^{13}C$ correlations compared to the U/Ca-$\delta^{18}O$ correlations (**Figures 3C,D**).

Uranium Speciation in Seawater

Figure 5 shows uranium speciation changes with pH in seawater at either a constant alkalinity or a constant DIC with stability constants from Guillaumont et al. (2003) and Endrizzi and Rao (2014). We see that the dominant uranium species is the uncharged $Ca_2UO_2(CO_3)_3(aq)$ (58.2%), followed by $MgUO_2(CO_3)_3^{2-}$ (19.1%) and $CaUO_2(CO_3)_3^{2-}$ (16.7%).

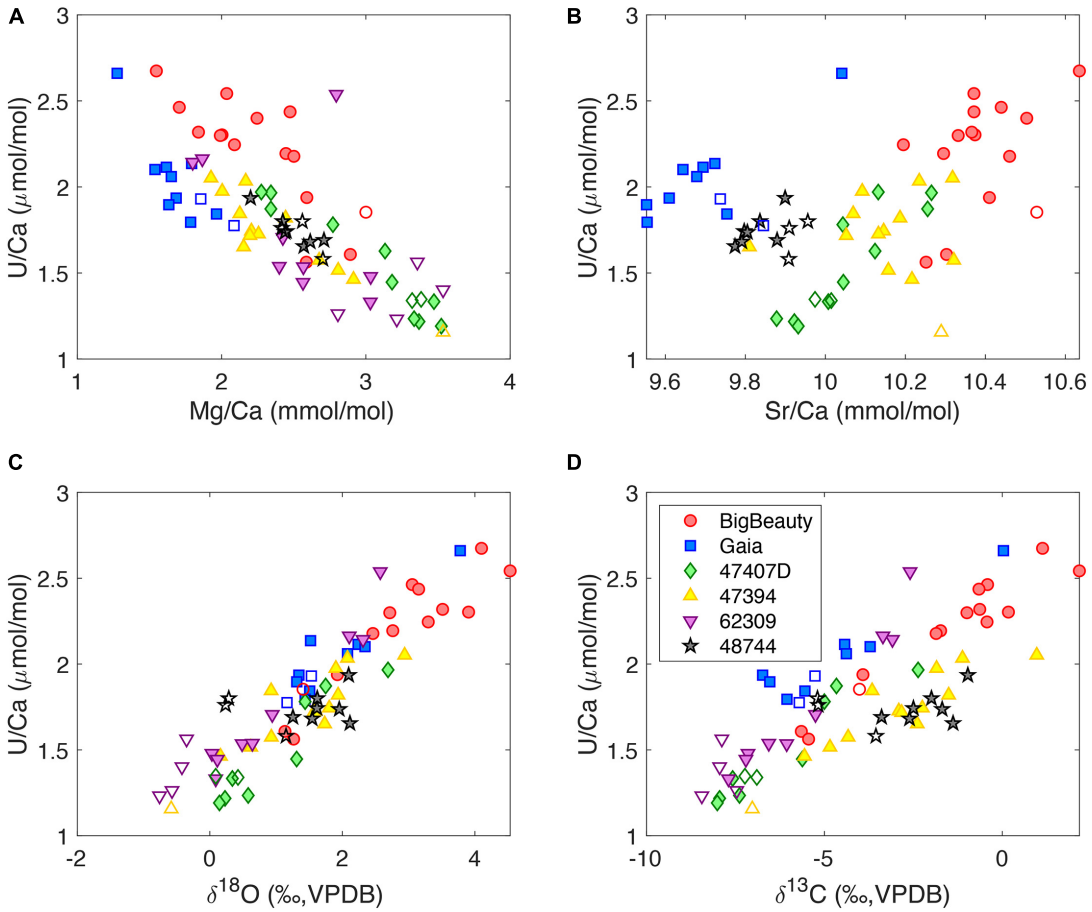

FIGURE 3 | U/Ca correlations with **(A)** Mg/Ca, **(B)** Sr/Ca, **(C)** $\delta^{18}O$ and **(D)** $\delta^{13}C$ in individual *D. dianthus* from micromilling. The filled symbols represent the secondary aragonite bands, while the open symbols represent COCs and COC-like bands. Coral 62309 was measured at St. Andrews while the others were measured at Caltech. There are analytical problems with Sr/Ca for 62309 and its Sr/Ca data are not shown.

$UO_2(CO_3)_3^{4-}$, the dominant species in freshwater at alkaline pH, only constitutes a minor fraction (6.0%) of total uranium under seawater conditions. All other uranium species have negligible contributions to total uranium. Over much of the pH range covered, there is little change in the relative contributions of the dominant uranium species because we assumed constant $[Ca^{2+}]$ and $[Mg^{2+}]$ in the calculations.

DISCUSSION

Uranium Speciation Changes in the Biomineralization Process

In contrast to seawater with constant $[Ca^{2+}]$ and $[Mg^{2+}]$, there are more dynamic changes in the carbonate chemistry and $[Ca^{2+}]$ in the ECF during the biomineralization process, which can significantly impact the uranium speciation. **Figure 6** shows uranium speciation changes in the ECF in response to the internal pH up-regulation by the alkalinity pump at different f_{Ca} values. Changing f_{Ca} significantly alters the $[Ca^{2+}]$ dynamics in the ECF and has strong impacts on the speciation of uranium. When $f_{Ca} = 1$, the Ca^{2+} pump is balanced by aragonite precipitation in the model at different pump rates, maintaining a relatively constant $[Ca^{2+}]$ in the ECF and therefore small changes in U speciation, until $UO_2(OH)_3^-$ takes over at high pH. In contrast, when $f_{Ca} = 0$, Ca^{2+} is removed from the ECF by aragonite precipitation with supply coming only from seawater. Therefore, $[Ca^{2+}]$ decreases in the ECF for this end member scenario as the alkalinity pump and precipitation rate increase, causing a decrease in $Ca_2UO_2(CO_3)_3$ and an increase in $MgUO_2(CO_3)_3^{2-}$ at higher pH. We expect such changes in uranium speciation to influence the amount of uranium incorporated into the coral skeleton, depending on the species that is preferentially taken into the aragonite lattice.

Uranium Incorporation Mechanism

Given the sensitivity of uranium speciation to $[Ca^{2+}]$ and the carbonate chemistry of the solution, the U/Ca proxy is expected to be strongly influenced by the biomineralization process. X-ray absorption experiments in synthetic carbonates showed that uranyl in aragonite has the same bonding configuration as aqueous $UO_2(CO_3)_3^{4-}$, suggesting intact

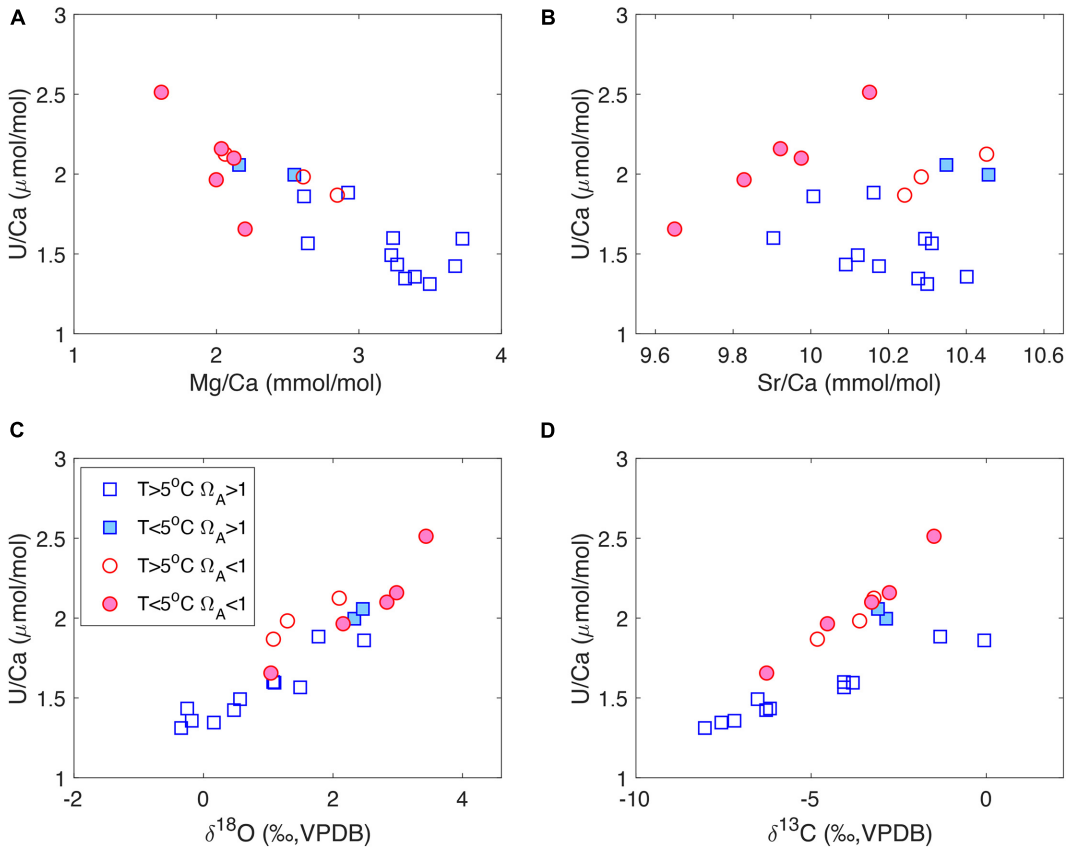

FIGURE 4 | U/Ca correlations with **(A)** Mg/Ca, **(B)** Sr/Ca, **(C)** $\delta^{18}O$ and **(D)** $\delta^{13}C$ in bulk *D. dianthus* samples listed in **Table 1**. The corals are grouped according to their environmental conditions, with a threshold temperature of 5°C and aragonite saturation state (Ω_A) of 1.

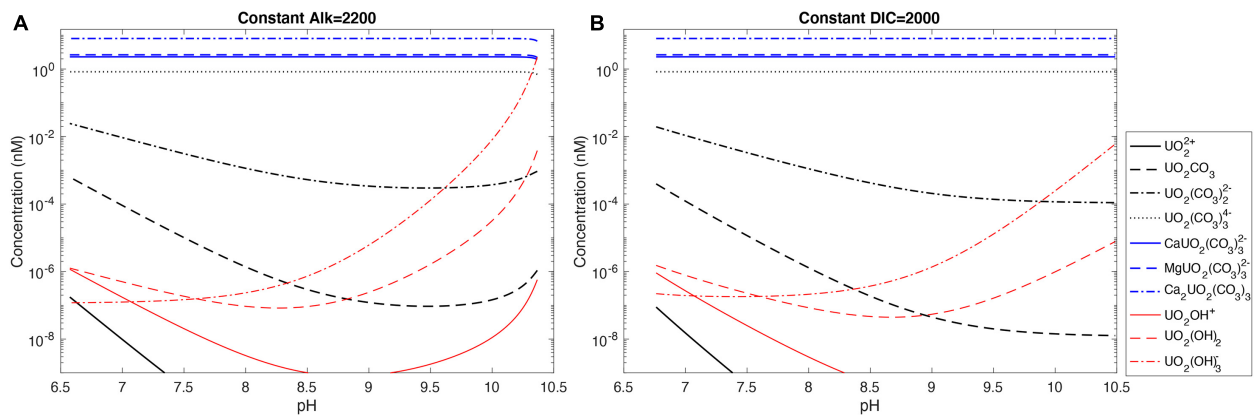

FIGURE 5 | Uranium speciation in seawater with pH at **(A)** constant alkalinity of 2,200 μeq/kg and **(B)** constant DIC of 2,000 μmol/kg. A total uranium concentration of 13.8 nmol/kg is used for the calculations.

incorporation of the whole unit in place of a Ca polyhedron with three CO_3^{2-} units (Reeder et al., 2000). These precipitation experiments, however, were performed in low ionic strength solutions without significant contributions of the Ca-UO_2-CO_3 and Mg-UO_2-CO_3 complexes to the uranium speciation. Aragonite precipitation experiments in seawater by DeCarlo et al. (2015) revealed a dependence of the uranium distribution coefficient on [CO_3^{2-}] and suggested uranium speciation changes as the most likely mechanism, although their speciation calculations do not consider the Ca-UO_2-CO_3 and Mg-UO_2-CO_3 complexes, either. Recent work on uranium isotopes in synthetic carbonates grown in NaCl solution found very

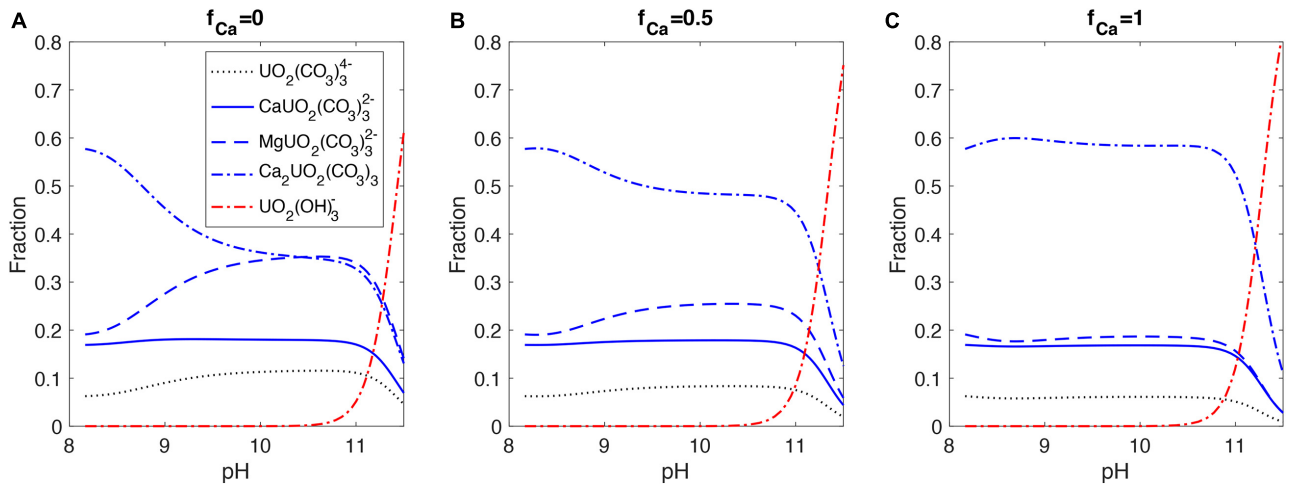

FIGURE 6 | Uranium speciation with pH in the ECF from the coral biomineralization model. The three panels correspond to different fractions of Ca^{2+} (f_{Ca}) in the alkalinity pump (**[A]** f_{Ca} = 0, **[B]** f_{Ca} = 0.5, **[C]** f_{Ca} = 1). Uranium speciation is calculated with steady state [Ca^{2+}], [Mg^{2+}], and carbonate chemistry simulated by the model corresponding to prescribed alkalinity pump rates. [Mg^{2+}] is almost constant in the model due to very limited removal by precipitation ($D_{Mg} << 1$ in aragonite).

small to no fractionation between the solution and the mineral (Chen X. et al., 2016). Chen X. et al. (2016) suggested the observed small $\delta^{238}U$ enrichment (0.11‰) in aragonite relative to aqueous uranium could be a result of the preferential incorporation of the charged complexes [$CaUO_2(CO_3)_3^{2-}$ and $MgUO_2(CO_3)_3^{2-}$] that are expected to be enriched in ^{238}U. However, the ^{238}U enrichment was observed in only one aragonite experiment, and their later work on biogenic carbonates found little fractionation between multiple coral species and seawater (Chen X. et al., 2018), suggesting either no particular preference for the incorporation of any uranium species or little isotope fractionation between the species. We can further test these ideas with the observed tracer correlations in deep-sea corals.

Among the tracer correlations observed in *D. dianthus*, the most robust one is between U/Ca and $\delta^{18}O$ in both the micromill and bulk data (**Figures 3C**, **4C**). The positive U/Ca-$\delta^{18}O$ correlations are almost identical for the micromill and bulk data. The sign of the correlation suggests a depletion in uranium incorporation with lower $\delta^{18}O$, which corresponds to higher alkalinity pump rates and ECF pH. A growth rate effect cannot explain a U/Ca decrease with higher pH, since the distribution coefficient for uranium is expected to increase at higher growth rates in aragonite (Gabitov et al., 2008). Following Equation (3), a decrease in uranium incorporation at higher pH is most likely a result of changes in total uranium concentration and the abundance of the preferentially incorporated uranium species relative to Ca^{2+} in the ECF. We can explore which uranium species is preferentially incorporated by comparing observed tracer correlations with model results.

Figure 7 shows the data-model comparison for U/Ca correlations with other tracers under different uranium incorporation scenarios. We see that in order to get the correct signs of tracer correlations in the data, the distribution coefficient for uranium (D_U) has to be greater than 1, regardless of the uranium species incorporated. With $D_U > 1$, uranium is preferentially removed from the ECF over Ca, causing a decrease in U/Ca at higher alkalinity pump rates and ECF pH. With such a distillation process, U/Ca in corals have lower values and are more sensitive to [CO_3^{2-}] than inorganic aragonite (DeCarlo et al., 2015). In terms of the uranium species incorporated into the coral skeleton, we get a better match between the data and the model when we either consider total uranium (all uranium species are incorporated without particular preference) or the dominant species $Ca_2UO_2(CO_3)_3$, as compared to the other species (**Figure 7**). Between U_{total} and $Ca_2UO_2(CO_3)_3$, we see that the model parameter set with $Ca_2UO_2(CO_3)_3$ incorporation at f_{Ca} = 0 fits most of the features in U/Ca correlations with $\delta^{18}O$, Mg/Ca, and Sr/Ca (**Figures 7E,J,O**). For U_{total}, the f_{Ca} values required to fit the U/Ca-$\delta^{18}O$ and U/Ca-Mg/Ca correlations are different, and the model cannot create the U/Ca-Sr/Ca slope in the majority of the data regardless of the f_{Ca} value (**Figures 7A,F,K**). As a result, our tracer data and biomineralization model favors $Ca_2UO_2(CO_3)_3$ as the uranium species that is preferentially incorporated into the coral skeletons. $Ca_2UO_2(CO_3)_3$ has several advantages in terms of incorporation into the aragonite lattice. Besides being the dominant aqueous uranium species in seawater, it is also uncharged and has a symmetric structure that is similar to the arrangement of Ca^{2+} and CO_3^{2-} ions in the aragonite lattice (Wu et al., 2016). This may allow it to substitute for three whole $CaCO_3$ unit cells without much distortion in the structure of the mineral. This could explain the lack of uranium isotope fractionation between coral skeletons and seawater observed by Chen X. et al. (2018). Stoichiometrically, such a substitution is equivalent to a UO_2^{2+}-for-Ca^{2+} swap, which may also explain why the calculations by Min et al. (1995) were able to

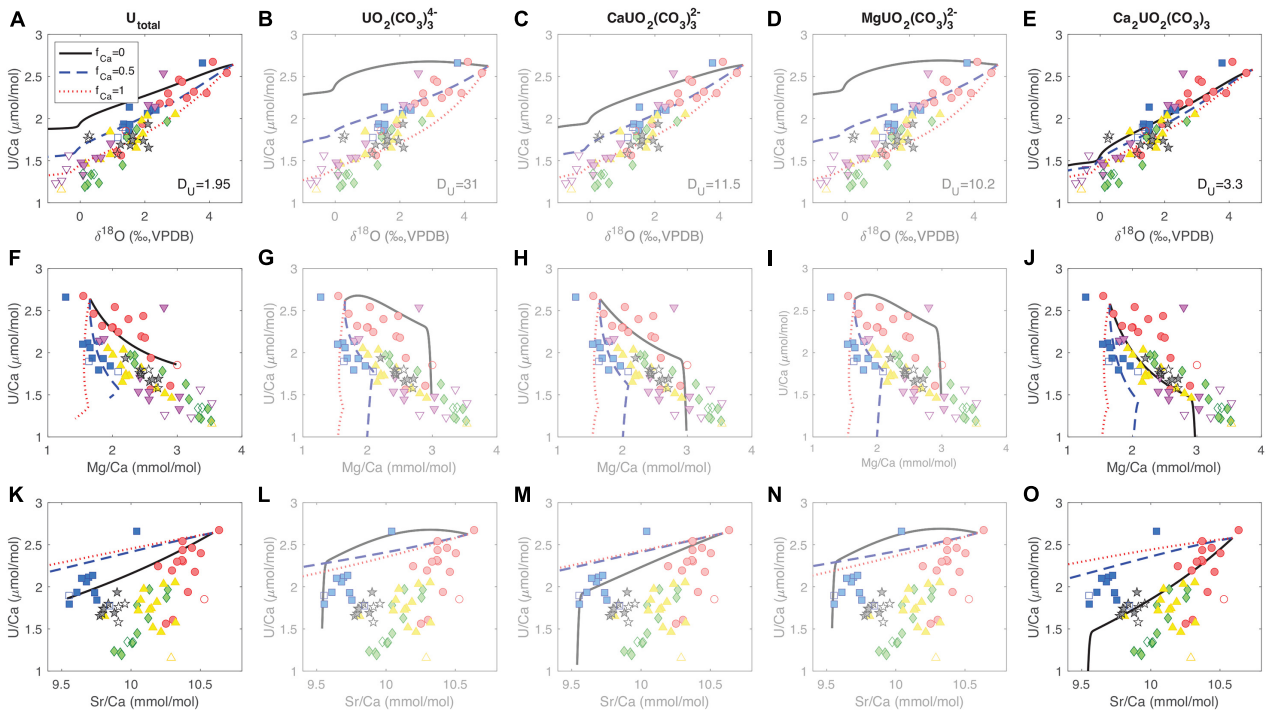

FIGURE 7 | Comparison of tracer correlation patterns between the data and the model. Each row **(A–E,F–J,K–O)** shows a different tracer correlation from the micromill data as in **Figure 3**. Each column **(AFK,BGL,CHM,DIN,EJO)** corresponds to tracer correlations predicted by the model assuming a certain uranium species that gets incorporated into the coral skeleton. The three curves correspond to different f_{Ca} values in each panel (f_{Ca} = 0 black solid, f_{Ca} = 0.5 blue dashed, f_{Ca} = 1 red dotted). The uranium distribution coefficients (D_U) required to fit the range in U/Ca is listed in Row 1 corresponding to each species. Transparency shading is added to Columns 2–4 to emphasize the model cases with U_{total} and $Ca_2UO_2(CO_3)_3$ that better fit the pattern in the data.

predict the temperature sensitivity of U/Ca based on a simple UO_2^{2+}-for-Ca^{2+} exchange reaction.

In addition to diagnosing the uranium species preferentially incorporated, the data-model comparison also suggests that the tracer correlation patterns are best explained by the f_{Ca} = 0 case. This is most clearly reflected in the U/Ca-Mg/Ca and U/Ca-Sr/Ca correlations, where f_{Ca} = 0 yields the slopes that best match the data. When f_{Ca} = 0.5 or 1, the simulated range in Mg/Ca is too small while the range in Sr/Ca is too large for the same amount of U/Ca changes, and is related to the different distribution coefficients for these two elements in aragonite ($D_{Mg} < < 1$, $D_{Sr} > 1$), which has been previously suggested (Gaetani and Cohen, 2006; Gagnon et al., 2007; Gaetani et al., 2011) and will be detailed in a separate paper. In brief, the observed tracer correlations point toward a case of limited Ca^{2+} pumping (low f_{Ca}) in the cross-membrane alkalinity flux to the ECF in *D. dianthus*. Given a 5:1 Ca:DIC ratio (and ~100:1 Ca^{2+}:CO_3^{2-} ratio) in seawater, it is a better strategy for the corals to elevate DIC and pH in the ECF to facilitate precipitation with alkalinity pumps that are more efficient than Ca-ATPase, instead of spending a lot of energy in elevating $[Ca^{2+}]_{ECF}$. Quantifying the relative importance of various alkalinity pumps in different marine calcifying organisms is an interesting target for future culture experiments.

Finally, it should be noted that our model is not able to fit all the features in the tracer data. The misfit is mostly seen at the high pH end with depleted $\delta^{18}O$, high Mg/Ca, and low U/Ca (**Figure 7**). There is a kink in most model curves in **Figure 7** related to drastic carbonate chemistry changes as the pH is elevated above pK_{a2} of the carbonate system, which is also reflected in the $\delta^{18}O$-$\delta^{13}C$ correlation in the COCs (Adkins et al., 2003; Chen S. et al., 2018). It is possible that the COCs have a different incorporation mechanism for minor and trace elements, as evidenced by their unique elemental compositions and tracer correlations (high Mg/Ca, low B/Ca, and U/Ca, intermediate Sr/Ca, **Figure 2**). This could complicate the empirical tracer calibrations in bulk coral samples. It is also possible that the exact uranium incorporation mechanism in aragonite is more complicated than our simple model can currently account for.

Implications for U/Ca as a [CO_3^{2-}] Proxy

With the micromill data and the biomineralization model, we are able to find a scenario that explains most of the tracer data in *D. dianthus*, with $Ca_2UO_2(CO_3)_3$ as the incorporated uranium species and limited Ca^{2+} pumping (low f_{Ca}). This could give us clues to the impact of the biomineralization process on empirical tracer calibrations for U/Ca. The observation that U/Ca is slightly better correlated with $\Delta[CO_3^{2-}]$ than $[CO_3^{2-}]$ (**Figures 1C,D**) suggests that the saturation state of seawater plays a role in uranium incorporation. We see from bulk tracer correlations that corals living in high saturation seawater tend to have lower $\delta^{18}O$, higher Mg/Ca and lower U/Ca compared to their

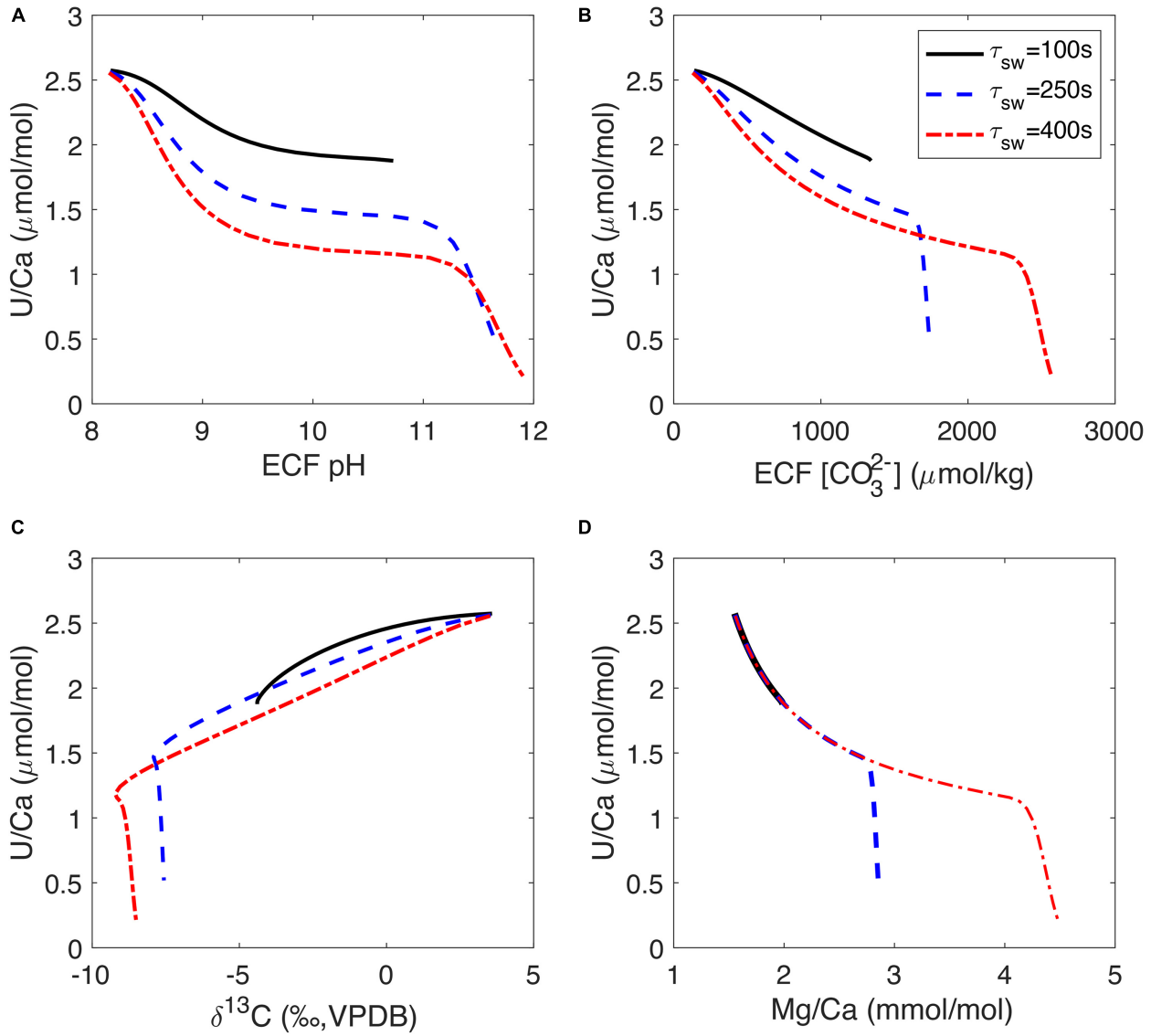

FIGURE 8 | U/Ca model sensitivity to seawater turnover timescale (τ_{sw}) in the ECF. Panels **(A–D)** show U/Ca relations with ECF pH, ECF [CO_3^{2-}], skeleton $\delta^{13}C$ and Mg/Ca respectively. In panel **(D)**, the three curves overlap on the low Mg/Ca high U/Ca end. Three curves correspond to different seawater turnover timescales in each panel simulated over the same range of alkalinity pump rates. The model curves are generated with f_{Ca} = 0 and assuming $Ca_2UO_2(CO_3)_3$ is the incorporated uranium species (as in **Figure 7** Column 5).

counterparts from low saturation seawater (**Figure 4**), suggesting the corals have overall higher alkalinity pump rates when the environmental conditions are favorable for calcification. The negative U/Ca-[CO_3^{2-}] correlation from bulk *D. dianthus* samples is most likely a result of the response of the strength of the alkalinity pump to the ambient environment. On the other hand, the scatter in the U/Ca-[CO_3^{2-}] correlation is likely a result of the differences in the magnitude of internal pH elevation in individual corals that was randomly sampled in the bulk powder, given a twofold or more change in U/Ca in individual corals. For example, the two corals from the Mediterranean Sea have higher U/Ca than the U/Ca-[CO_3^{2-}] trend defined by other corals would suggest (**Figure 1C**). However, the bulk $\delta^{18}O$ of these two corals are also closer to equilibrium than the other corals from supersaturated seawater, suggesting overall lower alkalinity pump rates. This may be the result of a sampling bias, but can also be related to the corals lowering the energetic cost of alkalinity pumping when the growth environment is favorable for calcification. A similar observation can be made on *Lophelia pertusa* (recently reclassified as *Desmophyllum pertusum* by Addamo et al., 2016), another deep-sea coral species. Although U/Ca in *L. pertusa* was found to be better correlated with pH than with [CO_3^{2-}] by Raddatz et al. (2014), the Mediterranean samples show a different U/Ca-[CO_3^{2-}] relation from their North Atlantic counterparts. While pH and [CO_3^{2-}] are often strongly correlated in seawater, Mediterranean seawater has very

different physical and chemical properties from the open ocean and thus a different pH-[CO_3^{2-}] relation, which is manifested by higher [CO_3^{2-}] at similar pH values (Flögel et al., 2014) and influences the U/Ca calibrations in both *D. dianthus* and *L. pertusa*. Flögel et al. (2014) also suggested that high DIC in the Mediterranean Sea may negatively impact the growth of *L. pertusa* and limit its colony size, which could also affect *D. dianthus* if they share a similar calcification mechanism. Overall, the stronger correlations for bulk U/Ca with $\delta^{18}O$ and Mg/Ca compared to ambient [CO_3^{2-}] indicate dominant control by the biomineralization process on the U/Ca proxy. This also supports the use of U/Ca as a normalizer for the vital effects in the development of better proxies such as the Sr-U thermometer in corals (DeCarlo et al., 2016).

While the strong biological control on U incorporation complicates the application of the U/Ca proxy, the observed correlations between U/Ca and other tracers may provide insights into the response of the coral biomineralization process to the environmental conditions. We see in **Figure 7** that increasing the fraction of Ca^{2+} in the alkalinity pump (f_{Ca}) can cause changes in U/Ca variability relative to other tracers and generate different tracer correlation slopes. Another way to change the sensitivity of U/Ca to the alkalinity pump in our model is to change the seawater turnover timescale (τ_{sw}). **Figure 8** shows the sensitivity of U/Ca to ECF pH and [CO_3^{2-}] as well as U/Ca correlations with $\delta^{13}C$ and Mg/Ca at different seawater turnover rates. We see that U/Ca is more sensitive to ECF pH and [CO_3^{2-}] at low pump rates, causing a concave-down trend in the correlations (**Figures 8A,B**). The low U/Ca sensitivity to ECF pH and [CO_3^{2-}] at high pump rates could explain the observation of low U/Ca extending beyond the COCs in *D. dianthus* (Robinson et al., 2006). U/Ca sensitivity to pH and [CO_3^{2-}] increases when seawater turnover is slowed down (longer τ_{sw}), and the corresponding U/Ca-$\delta^{13}C$ slope is also steeper (**Figure 8C**). The U/Ca-Mg/Ca correlation trend is not influenced by τ_{sw} in our simple model, but the range of variability in U/Ca and Mg/Ca also increases with τ_{sw} (**Figure 8D**). As seawater turnover is slowed down, the ECF is more like a closed system that increases the distillation of uranium relative to Ca^{2+} and causes larger changes in U/Ca. The change in U/Ca-$\delta^{13}C$ slope in the bulk *D. dianthus* data (**Figure 4D**) could be a result of individual corals adapting to their growth environment by changing their calcification strategies. Corals living in high saturation seawater tend to have a relatively fast seawater turnover and low f_{Ca} in the alkalinity pump while pumping to relatively high pH in the ECF, all of which tend to reduce U/Ca sensitivity to the biomineralization process. On the contrary, corals living in a low saturation environment would slow down the turnover of the corrosive seawater and have to make up for the Ca^{2+} supply by increasing f_{Ca} in the alkalinity pump. In addition, the magnitude of pH elevation is likely more limited in corals from low saturation seawater (as shown by the range in stable isotopes), further increasing the sensitivity of U/Ca to the calcification dynamics. Such differences in biomineralization strategies can explain the general trend in the U/Ca proxy calibration (**Figure 1**), but also adds complexity to its potential paleoceanographic applications. A multi-proxy approach is required to fully disentangle the vital effects from environmental imprints in different geochemical tracers in deep-sea corals and other biogenic carbonates.

CONCLUSION

We have combined stable isotopes, Me/Ca ratios and a numerical model of coral calcification to study uranium incorporation in deep-sea corals. While bulk U/Ca in *D. dianthus* show statistically significant correlations with temperature and ambient [CO_3^{2-}], there is significant scatter in the empirical calibrations that is related to the biomineralization process. Given the strong tracer correlations between U/Ca, Mg/Ca, Sr/Ca, $\delta^{18}O$, and $\delta^{13}C$ both in the bulk samples and within the growth bands in individual corals, we suggest that the uncharged $Ca_2UO_2(CO_3)_3(aq)$ complex, the dominant uranium species in seawater, is likely the preferentially incorporated uranium species in coral skeletons. Deep-sea corals may also change their biomineralization strategies in response to the growth environment, including overall lower alkalinity pump rates, increases in the fraction of Ca^{2+} pumping as well as slower seawater turnover when the ambient seawater is less saturated. The empirical correlation between U/Ca and seawater [CO_3^{2-}] is mainly a result of changes in overall alkalinity pump rates, but can be complicated by the exact calcification strategy used by individual corals. We expect a multi-proxy approach that couples stable isotopes and Me/Ca ratios to better help us better understand the mechanisms of vital effects and use these tracers for paleoceanographic reconstructions.

DATA AVAILABILITY STATEMENT

The original contributions presented in the study are included in the article/**Supplementary Material**, further inquiries can be directed to the corresponding author/s.

AUTHOR CONTRIBUTIONS

SC, JR, and JA designed the research. SC prepared the coral samples. SC, EL, JR, and CC performed the geochemical analyses. SC, EL, JR, and JA analyzed the data. All authors contributed to the writing of the manuscript.

FUNDING

This research received funding from NSF grant OCE-1737404 awarded to JA and China Scholarship Council Ph.D. Scholarship 201508020007 awarded to SC. JR was supported by ERC Starting Grant 805246 OldCO2NewArchives.

ACKNOWLEDGMENTS

We would like to thank Jessica Crumpton-Banks, Jared Marske, and Grecia Ames for assistance in the lab. We would also like to thank Joe Stewart and Russell Day for providing standards

for the geochemical analyses. We are indebted to co-editors Guillaume Paris, AG, Claire Rollion-Bard, and Oscar Branson for consideration of our work in this special issue of biomineralization. The manuscript benefited from comments by two reviewers.

SUPPLEMENTARY MATERIAL

The Supplementary Material for this article can be found online at: https://www.frontiersin.org/articles/10.3389/feart.2021.641327/full#supplementary-material

REFERENCES

Addamo, A. M., Vertino, A., Stolarski, J., García-Jiménez, R., Taviani, M., and Machordom, A. (2016). Merging scleractinian genera: the overwhelming genetic similarity between solitary *Desmophyllum* and colonial *Lophelia*. *BMC Evol. Biol.* 16:108. doi: 10.1186/s12862-016-0654-8

Adkins, J. F., Boyle, E. A., Curry, W. B., and Lutringer, A. (2003). Stable isotopes in deep-sea corals and a new mechanism for "vital effects.". *Geochim. Cosmochim. Acta* 67, 1129–1143. doi: 10.1016/S0016-7037(02)01203-6

Al-Horani, F. A., Al-Moghrabi, S. M., and de Beer, D. (2003). The mechanism of calcification and its relation to photosynthesis and respiration in the scleractinian coral *Galaxea fascicularis*. *Mar. Biol.* 142, 419–426. doi: 10.1007/s00227-002-0981-8

Allen, K. A., Hönisch, B., Eggins, S. M., Haynes, L. L., Rosenthal, Y., and Yu, J. (2016). Trace element proxies for surface ocean conditions: a synthesis of culture calibrations with planktic foraminifera. *Geochim. Cosmochim. Acta* 193, 197–221. doi: 10.1016/j.gca.2016.08.015

Anagnostou, E., Sherrell, R. M., Gagnon, A., LaVigne, M., Field, M. P., and McDonough, W. F. (2011). Seawater nutrient and carbonate ion concentrations recorded as P/Ca, Ba/Ca, and U/Ca in the deep-sea coral *Desmophyllum dianthus*. *Geochim. Cosmochim. Acta* 75, 2529–2543. doi: 10.1016/j.gca.2011.02.019

Barnett, M. O., Jardine, P. M., Brooks, S. C., and Selim, H. M. (2000). Adsorption and transport of uranium(VI) in subsurface media. *Soil Sci. Soc. Am. J.* 64, 908–917. doi: 10.2136/sssaj2000.643908x

Barott, K. L., Perez, S. O., Linsmayer, L. B., and Tresguerres, M. (2015). Differential localization of ion transporters suggests distinct cellular mechanisms for calcification and photosynthesis between two coral species. *Am. J. Physiol. Regulat. Integrat. Compar. Physiol.* 309, R235–R246. doi: 10.1152/ajpregu.00052.2015

Barron, M. E., Thies, A. B., Espinoza, J. A., Barott, K. L., Hamdoun, A., and Tresguerres, M. (2018). A vesicular Na+/Ca2+ exchanger in coral calcifying cells. *PLoS One* 13:e0205367. doi: 10.1371/journal.pone.0205367

Blamart, D., Rollion−Bard, C., Meibom, A., Cuif, J.-P., Juillet−Leclerc, A., and Dauphin, Y. (2007). Correlation of boron isotopic composition with ultrastructure in the deep-sea coral Lophelia pertusa: Implications for biomineralization and paleo-pH. *Geochem. Geophys. Geosyst.* 8:12. doi: 10.1029/2007GC001686

Broecker, W. S. (1963). A preliminary evaluation of uranium series inequilibrium as a tool for absolute age measurement on marine carbonates. *J. Geophys. Res.* 68, 2817–2834. doi: 10.1029/JZ068i009p02817

Case, D. H., Robinson, L. F., Auro, M. E., and Gagnon, A. C. (2010). Environmental and biological controls on Mg and Li in deep-sea scleractinian corals. *Earth Planet. Sci. Lett.* 300, 215–225. doi: 10.1016/j.epsl.2010.09.029

Chen, S., Gagnon, A. C., and Adkins, J. F. (2018). Carbonic anhydrase, coral calcification and a new model of stable isotope vital effects. *Geochim. Cosmochim. Acta* 236, 179–197. doi: 10.1016/j.gca.2018.02.032

Chen, T., Robinson, L. F., Beasley, M. P., Claxton, L. M., Andersen, M. B., Gregoire, L. J., et al. (2016). Ocean mixing and ice-sheet control of seawater 234U/238U during the last deglaciation. *Science* 354, 626–629. doi: 10.1126/science.aag1015

Chen, X. (2020). Aqueous uranium speciation on U/Ca in foraminiferal calcite: the importance of minor species—$UO_2(CO_3)_2^{2-}$. *ACS Earth Space Chem.* 4, 2050–2060.

Chen, X., Romaniello, S. J., Herrmann, A. D., Samankassou, E., and Anbar, A. D. (2018). Biological effects on uranium isotope fractionation ($^{238}U/^{235}U$) in primary biogenic carbonates. *Geochim. Cosmochim. Acta.* 240, 1–10. doi: 10.1016/j.gca.2018.08.028

Chen, X., Romaniello, S. J., Herrmann, A. D., Wasylenki, L. E., and Anbar, A. D. (2016). Uranium isotope fractionation during coprecipitation with aragonite and calcite. *Geochim. Cosmochim. Acta* 188, 189–207. doi: 10.1016/j.gca.2016.05.022

Cheng, H., Adkins, J., Edwards, R. L., and Boyle, E. A. (2000). U-Th dating of deep-sea corals. *Geochim. Cosmochim. Acta* 64, 2401–2416. doi: 10.1016/S0016-7037(99)00422-6

Cutler, K. B., Edwards, R. L., Taylor, F. W., Cheng, H., Adkins, J., Gallup, C. D., et al. (2003). Rapid sea-level fall and deep-ocean temperature change since the last interglacial period. *Earth Planet. Sci. Lett.* 206, 253–271. doi: 10.1016/S0012-821X(02)01107-X

de Nooijer, L. J., Toyofuku, T., and Kitazato, H. (2009). Foraminifera promote calcification by elevating their intracellular pH. *Proc. Natl. Acad. Sci.* 106, 15374–15378. doi: 10.1073/pnas.0904306106

DeCarlo, T. M., Gaetani, G. A., Cohen, A. L., Foster, G. L., Alpert, A. E., and Stewart, J. A. (2016). Coral Sr-U thermometry. *Paleoceanography* 31, 626–638. doi: 10.1002/2015PA002908

DeCarlo, T. M., Gaetani, G. A., Holcomb, M., and Cohen, A. L. (2015). Experimental determination of factors controlling U/Ca of aragonite precipitated from seawater: implications for interpreting coral skeleton. *Geochim. Cosmochim. Acta* 162, 151–165. doi: 10.1016/j.gca.2015.04.016

Djogić, R., Sipos, L., and Branica, M. (1986). Characterization of uranium(VI) in seawater1. *Limnol. Oceanogr.* 31, 1122–1131. doi: 10.4319/lo.1986.31.5.1122

Dong, W., and Brooks, S. C. (2006). Determination of the formation constants of ternary complexes of uranyl and carbonate with alkaline earth metals (Mg2+, Ca2+, Sr2+, and Ba2+) using anion exchange method. *Environ. Sci. Technol.* 40, 4689–4695. doi: 10.1021/es0606327

Edwards, L. R., Chen, J. H., and Wasserburg, G. J. (1987). 238U234U230Th232Th systematics and the precise measurement of time over the past 500,000 years. *Earth Planet. Sci. Lett.* 81, 175–192. doi: 10.1016/0012-821X(87)90154-3

Endrizzi, F., and Rao, L. (2014). Chemical speciation of uranium(VI) in marine environments: complexation of calcium and magnesium ions with [(UO2)(CO3)3](4-) and the effect on the extraction of uranium from seawater. *Chem. (Weinheim Bergstr. Germ.)* 20, 14499–14506. doi: 10.1002/chem.201403262

Flögel, S., Dullo, W.-C. h. r., Pfannkuche, O., Kiriakoulakis, K., and Rüggeberg, A. (2014). Geochemical and physical constraints for the occurrence of living cold-water corals. *Deep Sea Res. Part II Top. Stud. Oceanogr.* 99, 19–26. doi: 10.1016/j.dsr2.2013.06.006

Gabitov, R. I., Gaetani, G. A., Watson, E. B., Cohen, A. L., and Ehrlich, H. L. (2008). Experimental determination of growth rate effect on U6+ and Mg2+ partitioning between aragonite and fluid at elevated U6+ concentration. *Geochim. Cosmochim. Acta* 72, 4058–4068. doi: 10.1016/j.gca.2008.05.047

Gaetani, G. A., and Cohen, A. L. (2006). Element partitioning during precipitation of aragonite from seawater: a framework for understanding paleoproxies. *Geochim. Cosmochim. Acta* 70, 4617–4634. doi: 10.1016/j.gca.2006.07.008

Gaetani, G. A., Cohen, A. L., Wang, Z., and Crusius, J. (2011). Rayleigh-based, multi-element coral thermometry: a biomineralization approach to developing climate proxies. *Geochim. Cosmochim. Acta* 75, 1920–1932. doi: 10.1016/j.gca.2011.01.010

Gagnon, A. C., Adkins, J. F., Fernandez, D. P., and Robinson, L. F. (2007). Sr/Ca and Mg/Ca vital effects correlated with skeletal architecture in a scleractinian deep-sea coral and the role of Rayleigh fractionation. *Earth Planet. Sci. Lett.* 261, 280–295. doi: 10.1016/j.epsl.2007.07.013

Guillaumont, R., Mompean, F. J., and Oecd Nuclear Energy Agency, (Eds.) (2003). *Update on the Chemical Thermodynamics of Uranium, Neptunium, Plutonium, Americium and Technetium*. Amsterdam: Elsevier.

Hathorne, E. C., Gagnon, A., Felis, T., Adkins, J., Asami, R., Boer, W., et al. (2013). Interlaboratory study for coral Sr/Ca and other element/Ca ratio measurements. *Geochem. Geophys. Geosyst.* 14, 3730–3750. doi: 10.1002/ggge.20230

Inoue, M., Suwa, R., Suzuki, A., Sakai, K., and Kawahata, H. (2011). Effects of seawater pH on growth and skeletal U/Ca ratios of *Acropora digitifera* coral polyps. *Geophys. Res. Lett.* 38, 12. doi: 10.1029/2011GL047786

Jokiel, P. L. (2013). Coral reef calcification: carbonate, bicarbonate and proton flux under conditions of increasing ocean acidification. *Proc. R. Soc. B Biol. Sci.* 280:1764. doi: 10.1098/rspb.2013.0031

Keul, N., Langer, G., Nooijer, L. J., de Nehrke, G., Reichart, G.-J., and Bijma, J. (2013). Incorporation of uranium in benthic foraminiferal calcite reflects seawater carbonate ion concentration. *Geochem. Geophys. Geosyst.* 14, 102–111. doi: 10.1029/2012GC004330

Key, R. M., Olsen, A., van Heuven, S., Lauvset, S. K., Velo, A., Lin, X., et al. (2015). *Global Ocean Data Analysis Project, Version 2 (GLODAPv2) [Miscellaneous]. ORNL/CDIAC-162, NDP-093.* Ridge, TN: Carbon Dioxide Information Analysis Center, Oak Ridge National Laboratory. doi: 10.3334/CDIAC/OTG

Langmuir, D. (1978). Uranium solution-mineral equilibria at low temperatures with applications to sedimentary ore deposits. *Geochim. Cosmochim. Acta* 42(6 Part A), 547–569. doi: 10.1016/0016-7037(78)90001-7

Meece, D. E., and Benninger, L. K. (1993). The coprecipitation of Pu and other radionuclides with CaCO3. *Geochim. Cosmochim. Acta* 57, 1447–1458. doi: 10.1016/0016-7037(93)90005-H

Millero, F. J. (2010). Carbonate constants for estuarine waters. *Mar. Freshw. Res.* 61, 139–142. doi: 10.1071/MF09254

Min, R. G., Edwards, L. R., Taylor, F. W., Recy, J., Gallup, C. D., and Warren Beck, J. (1995). Annual cycles of UCa in coral skeletons and UCa thermometry. *Geochim. Cosmochim. Acta* 59, 2025–2042. doi: 10.1016/0016-7037(95)00124-7

Olsen, A., Key, R. M., Heuven, S., van Lauvset, S. K., Velo, A., Lin, X., et al. (2016). The global ocean data analysis project version 2 (GLODAPv2) – an internally consistent data product for the world ocean. *Earth Syst. Sci. Data* 8, 297–323. doi: 10.5194/essd-8-297-2016

Raddatz, J., Rüggeberg, A., Flögel, S., Hathorne, E. C., Liebetrau, V., Eisenhauer, A., et al. (2014). The influence of seawater pH on U / Ca ratios in the scleractinian cold-water coral *Lophelia pertusa*. *Biogeosciences* 11, 1863–1871. doi: 10.5194/bg-11-1863-2014

Raitzsch, M., Kuhnert, H., Hathorne, E. C., Groeneveld, J., and Bickert, T. (2011). U/Ca in benthic foraminifers: a proxy for the deep-sea carbonate saturation. *Geochem. Geophys. Geosyst.* 12:6. doi: 10.1029/2010GC003344

Reeder, R. J., Nugent, M., Lamble, G. M., Tait, C. D., and Morris, D. E. (2000). Uranyl incorporation into calcite and aragonite: XAFS and luminescence studies. *Environ. Sci. Technol.* 34, 638–644. doi: 10.1021/es990981j

Reeder, R. J., Nugent, M., Tait, C. D., Morris, D. E., Heald, S. M., Beck, K. M., et al. (2001). Coprecipitation of uranium(VI) with calcite: XAFS, micro-XAS, and luminescence characterization. *Geochim. Cosmochim. Acta* 65, 3491–3503. doi: 10.1016/S0016-7037(01)00647-0

Robinson, L. F., Adkins, J. F., Fernandez, D. P., Burnett, D. S., Wang, S.-L., Gagnon, A. C., et al. (2006). Primary U distribution in scleractinian corals and its implications for U series dating. *Geochem. Geophys. Geosyst.* 7:5. doi: 10.1029/2005GC001138

Robinson, L. F., Adkins, J. F., Frank, N., Gagnon, A. C., Prouty, N. G., Brendan Roark, E., et al. (2014). The geochemistry of deep-sea coral skeletons: a review of vital effects and applications for palaeoceanography. *Deep Sea Res Part II Top. Stud. Oceanogr.* 99, 184–198. doi: 10.1016/j.dsr2.2013.06.005

Rollion-Bard, C., Blamart, D., Cuif, J.-P., and Dauphin, Y. (2010). In situ measurements of oxygen isotopic composition in deep-sea coral, *Lophelia pertusa*: re-examination of the current geochemical models of biomineralization. *Geochim. Cosmochim. Acta* 74, 1338–1349. doi: 10.1016/j.gca.2009.11.011

Rollion-Bard, C., Chaussidon, M., and France-Lanord, C. (2003). PH control on oxygen isotopic composition of symbiotic corals. *Earth Planet. Sci. Lett.* 215, 275–288. doi: 10.1016/S0012-821X(03)00391-1

Russell, A. D., Hönisch, B., Spero, H. J., and Lea, D. W. (2004). Effects of seawater carbonate ion concentration and temperature on shell U, Mg, and Sr in cultured planktonic foraminifera. *Geochim. Cosmochim. Acta* 68, 4347–4361. doi: 10.1016/j.gca.2004.03.013

Shen, G. T., and Dunbar, R. B. (1995). Environmental controls on uranium in reef corals. *Geochim. Cosmochim. Acta* 59, 2009–2024. doi: 10.1016/0016-7037(95)00123-9

Sinclair, D. J. (2005). Correlated trace element "vital effects" in tropical corals: a new geochemical tool for probing biomineralization. *Geochim. Cosmochim. Acta* 69, 3265–3284. doi: 10.1016/j.gca.2005.02.030

Stewart, J. A., Anagnostou, E., and Foster, G. L. (2016). An improved boron isotope pH proxy calibration for the deep-sea coral *Desmophyllum dianthus* through sub-sampling of fibrous aragonite. *Chem. Geol.* 447, 148–160. doi: 10.1016/j.chemgeo.2016.10.029

Toyofuku, T., Matsuo, M. Y., de Nooijer, L. J., Nagai, Y., Kawada, S., Fujita, K., et al. (2017). Proton pumping accompanies calcification in foraminifera. *Nat. Commun.* 8:14145. doi: 10.1038/ncomms14145

Venn, A., Tambutté, E., Holcomb, M., Allemand, D., and Tambutté, S. (2011). Live tissue imaging shows reef corals elevate pH under their calcifying tissue relative to seawater. *PLoS One* 6:e20013. doi: 10.1371/journal.pone.0020013

Wu, W., Priest, C., Zhou, J., Peng, C., Liu, H., and Jiang, D.-E. (2016). Solvation of the Ca2UO2(CO3)3 complex in seawater from classical molecular dynamics. *J. Phys. Chem. B* 120, 7227–7233. doi: 10.1021/acs.jpcb.6b05452

York, D., Evensen, N. M., Martínez, M. L., and De Basabe Delgado, J. (2004). Unified equations for the slope, intercept, and standard errors of the best straight line. *Am. J. Phys.* 72, 367–375. doi: 10.1119/1.1632486

Zoccola, D., Tambutté, E., Kulhanek, E., Puverel, S., Scimeca, J.-C., Allemand, D., et al. (2004). Molecular cloning and localization of a PMCA P-type calcium ATPase from the coral *Stylophora pistillata*. *Biochim. Biophys. Acta (BBA) Biomembr.* 1663, 117–126. doi: 10.1016/j.bbamem.2004.02.010

Conflict of Interest: The authors declare that the research was conducted in the absence of any commercial or financial relationships that could be construed as a potential conflict of interest.

The handling editor declared a past co-authorship with JA and JR.